ISSN: 0067-2904

Electromagnetic Form Factors for ^{7,9,11}Be Isotopes with Exact Center of Mass Correction

M. H. Hawi *, Z. A. Dakhil
Department of Physics, College of Science, University of Baghdad, Baghdad, IRAQ

Received: 10/10/2020 Accepted: 23/3/2021

Abstract

The shell model calculations with Cohen-Kurath (C-K) interaction were carried out to investigate form factors of elastic transverse electron scattering, and magnetic dipole-moments of odd ^{7,9,11}Be isotopes. The effect of the exact value of center of mass correction was adopted to generate the magnetic form factors in Born approximation picture. The contribution of the higher 2*p*-shell configuration was included to reproduce the experimental data. A significant improvement was obtained in the present results with core-polarization (CP) effect through the effective g-factors. The occupancies percentage with respect to the valence nucleons was also calculated.

Keywords: Exotic nuclei, magnetic electron scattering, magnetic dipole moment.

عوامل التشكل الكهرومغناطيسية لنظائر البريليوم ^{7,9,11} Be مع تصحيح مركز الكتلة المضبوط

مرتضى هادي حاوي *، زاهدة أحمد دخيل
قسم الفيزياء، كلية العلوم، جامعة بغداد، بغداد-العراق

الخلاصة

اعتمدت حسابات أنموذج الأغلفة النووي باستخدام تفاعل كوهين–كوراث لدراسة عوامل التشكل المغناطيسية للإستطارة الإلكترونية المرنة وعزوم ثنائية القطب المغناطيسية لنظائر البريليوم Be 7,9,11 الفردية. تم تبني تأثير القيمة المضبوطة لتصحيح حركة مركز كتلة النواة لتعديل عوامل التشكل المغناطيسية وفق تقريب بورن. أدخلت مساهمات الأغلفة العالية 2 p–shell لتفسير المعطيات العملية. تحقق توافق ملموس بالنتائج الحالية بإدخال تأثير استقطاب القلب من خلال عوامل g–الفعالة. تم حساب النسبة المئوية لأعداد الأشغال نسبة إلى نويات التكافؤ لجميع النظائر قيد الدراسة.

1. Introduction

Elastic electron-nucleus scattering is one of the main probes to gain very clean information about the nuclear structure of stable nuclei and unstable nuclei because electrons and nucleons interact essentially with the electro-magnetic force. If energy of the

*Email: phymurteza@gmail.com

electron is sufficiently high, it can become a fairly good to precise probe to investigate the ultrastructure of the nucleus, insensitive to the effects of strong interaction. The benefits of electro-magnetic probes are shared by magnetic scattering, but there are still major variations compared to charge scattering. A detailed description of the advantages of using electron scattering in studying nuclear structure was given by Walecka et al. [1].

Elastic magnetic electron scattering has been widely used to study the valence structure of the nuclei near the stability line. Thus, the investigation of the properties of exotic nuclei has become one of the most important goals in nuclear physics. The magnetic moment is very sensitive to the single particle orbits occupied by the unpaired nucleons. Consequently, this quantity may also give a means to distinguish between spherical and deformed states. Analysis of neutron-rich nuclei shows unusual phenomena such as the weakening of closed shells and the creation of neutron halos. One of the most prominent features of neutron-rich nuclei is nuclear deformity, which can be studied by the measurements of electromagnetic moments and transitions [2,3]. Various studies of electron scattering have been performed to study the nuclear structure of exotic nuclei. Palit et al. [4] investigated the electromagnetic and nuclear inelastic of the halo nucleus ^{11}Be by a measurement of the one-neutron removal channel. The extracted dipole strength integrated from the neutron threshold up to 6.1 MeV excitation energy amounts to 0.90(6) e^2 fm^2. Marcucci et al. [5] performed Green's function Monte Carlo calculations of magnetic moments and M1 transitions for nuclei of mass number less than 7 including two-body meson exchange current (MEC) contributions. The results have very good agreement with the experimental data when contributions increase the A = 3,7 isovector magnetic moments by 16% and the A = 6,7 M1 transition rates by 17-34%. Dong and Ren [6] investigated the effects of the velocity-dependent force on the magnetic form factors and magnetic moments of individual nuclei. The diffraction structures beyond the existing experimental data were found after the contributions of the velocity-dependent force were included. Hammer and Phillips [7] used an effective field theory (EFT) to compute E1 transition and electric radii in the ^{11}Be halo nucleus. They fixed the request parameters of the Effective Field Theory (EFT) from measured data on $1/2^+$ and$1/2^-$ levels in ^{11}Be. Their results of B (E1) strength were in good agreement with the experimental data. The elastic scattering angular distributions for ^{7,9,10}Be isotopes were measured by Zamora et al. [8] at laboratory energies of 18.8, 26.0 and 23.2 MeV, using ^{12}C target. Analysis was carried out in terms of optical model potentials using Woods-Saxon and double-folding form factors. Fortune [9] examined the history and current state of knowledge of the structure of exotic light nuclei with Z from 2 to 4, from ^{7}He to ^{16}Be. He reviewed the empirical information and the models used for these nuclei. Special attention was given to the interplay among strengths, energies and microscopic structure. Sarriguren et al. [10,11] determined the form factors of the elastic magnetic electron scattering from odd-A nuclei in plane wave Born approximation using Skyrme HF+BCS method. The calculations were carried out on several stable nuclei. Their results for deformed formalism improved the agreement with experiment in deformed nuclei.

The present study aims to analyze the role of the center of mass correction on the transverse elastic electron scattering from ^{7,9,11}Be isotopes. The calculations were carried out through plane wave Born approximation for model space and other contributions, using Cohen-Kurath (C-K) interaction [12]. The correction for the center-of-mass motion introduced by Mihaila and Heisenberg [13] was adopted to generate the transverse form

factors. The calculations of this correction were based on the Translation Invariant Shell Model (TISM). The higher contributions of 2*p*-shell configuration were introduced. The core-polarization (CP) effects were included through the effective g-factors. The results were compared with available data of stable ^{9}Be nucleus and with other theoretical results.

2. Theory

The squared transverse form factors between initial J_i and final J_f nuclear states are given by [14]:

$$\left|F_J^T(q)\right|^2=\frac{4\pi}{Z^2(2J_i+1)}\left|\sum_{T=0,1}(-1)^{T_f-T_{zf}}\begin{pmatrix}T_f & T & T_i\\ -T_{Z_f} & M_T & T_{Z_i}\end{pmatrix}\left\langle\Gamma_f\left\|\hat{T}^{T}_{JT}(q)\right\|\Gamma_i\right\rangle\right|^2 \tag{1}$$

Where $\hat{T}_J(q)$ is the transverse multipole operator, the bracket $\begin{pmatrix}\cdot & \cdot & \cdot\\ \cdot & \cdot & \cdot\end{pmatrix}$ denotes the 3-*j* symbols and $\langle\|\ \|\rangle$ is the reduced matrix element, which are written as the product sum of the one-body density matrix (OBDM) elements times single particle transition matrix elements [15]:

$$\left\langle\Gamma_f\left\|\hat{T}^T_\Lambda\right\|\Gamma_i\right\rangle=\sum_{a,b}OBDM\ (\Gamma_i,\Gamma_f,a,b)\left\langle a\left\|\hat{T}^T_\Lambda\right\|b\right\rangle \tag{2}$$

Where $\Lambda=JT$ is the multipolarity and the states $\Gamma_i\equiv J_iT_i$ and $\Gamma_f\equiv J_fT_f$ are nucleus initial and final states. Calculations of the nuclear shell model are carried out using the OXBASH shell model code [16] to calculate (OBDM) elements.

The single nucleon finite size form factor [17] and the center of mass form factor [18] are provided by:

$$F_{fs}(q)=[1+(q/4.33)^2]^{-2}\quad F_{cm}(q)=e^{q^2b^2/4A} \tag{3}$$

Where *A* is the nuclear mass number and *b* is the size parameter of the harmonic-oscillator (HO). If these corrections are inserted into eq. (1), one can get:

$$\left|F_J^T(q)\right|^2=\frac{4\pi}{Z^2(2J_i+1)}\left|\sum_{T=0,1}(-1)^{T_f-T_{zf}}\begin{pmatrix}T_f & T & T_i\\ -T_{Zf} & M_T & T_{Zi}\end{pmatrix}\left\langle\Gamma_f\left\|\hat{T}^{T}_{J,T}(q)\right\|\Gamma_i\right\rangle\right|^2 \times\left|F_{c.m}(q)\right|^2\times\left|F_{f.s}(q)\right|^2 \tag{4}$$

The exact value of the center-of-mass correction in TISM, F_{int} [13] is:

$$F(\vec{q})=F_{c.m.}(\vec{q})\,F_{\text{int}}(\vec{q}) \tag{5}$$

$$F_{\text{int}}(\vec{q})=\left\langle\phi_\circ\left|\sum_k f_k(q^2)e^{i\vec{q}\cdot\vec{r}'_k}\right|\phi_\circ\right\rangle \tag{6}$$

Where $\phi_\circ$ is the translationally invariant ground state, $\vec{r}'_k$ is the distance from the center of mass to the k^{th} "point" nucleon, ($\vec{r}'_k=\vec{r}_k-\vec{R}_{c.m}$), *k = 1, 2, ...A-1* and $f_k(q^2)$ is the nucleon

form factor, which takes into account the finite size of the nucleon *k*. More details were presented by Mihaila and Heisenberg [13].

When the 1*p*-shell model space (MS) is extended to include the 2*p*-shell model space, the wave functions of the initial (i) and final (f) states will be written as [19]:

$$|i\rangle = \delta|i(1p)\rangle + \sqrt{1-\delta^2}|i(2p)\rangle \quad (7)$$

$$|f\rangle = \gamma|f(1p)\rangle + \sqrt{1-\gamma^2}|f(2p)\rangle \quad (8)$$

Where δ and γ are mixing parameters. Since the C-K interaction depends on the angular parts only, the same OBDM are used for both 1*p*- and 2*p*-shells.

For a state of total angular momentum *J*, the magnetic dipole-moment μ is [15]:

$$\mu = \sqrt{\frac{4\pi}{3}} \begin{pmatrix} J_i & 1 & J_i \\ -J_i & 0 & J_i \end{pmatrix} \left\langle J_i \left\| \sum_{k=1}^{n} \hat{O}_k(m1) \right\| J_i \right\rangle \quad (9)$$

The occupation numbers are given by [20]:

$$occ\#(j,t_z) = OBDM(a,b,t_z,J=0)\sqrt{\frac{2j+1}{2J_i+1}} \quad (10)$$

3. Results and Discussion

The transverse form factors and the magnetic dipole moments are considered as a good probe to investigate the nuclear structure of neutron (proton) rich nuclei.

According to the many-particle shell model, ^{7,9,11}Be isotopes are regarded as a core of ^{4}He plus the residual nucleons divided over $1p_{3/2}$, $1p_{1/2}$ orbits. Cohen-Kurath (C-K) interaction [12] was used to calculate the OBDM given in Eq. (2). The single – particle wave functions of harmonic oscillator (HO) potential with size parameter b were used. The size parameter b was calculated for each nucleus with mass number A as [21]:

$b = \sqrt{\frac{\hbar}{M_p\,\omega}}$; $\hbar\omega = 45\,A^{-1/3} - 25\,A^{-2/3}$, M_p is the mass of proton. The experimental information on the elastic transverse electron scattering form factors is available only for the stable ^{9}Be nucleus ($J^{\pi}T = 3/2^{-}1/2$) [17,22,23], and are dependent in comparison for all exotic Be-isotopes under consideration. The ^{7,11}Be isotopes were chosen to test the reliability of the theoretical model. The occupation numbers of the valence nucleons were also determined.

3.1 ^{9}Be stable nucleus ($J^{\pi}T = 3/2^{-}1/2$)

$(1s)^4$ inert core, $(1p)^5$ with C-K interaction [12] were the configurations used in the present work to characterize the ground state of ^{9}Be nucleus. A clear configuration mixture appeared with, 29.509% $(1p_{3/2})^3$ $(1p_{1/2})^2$, 20.834% $(1p_{3/2})^4$ $(1p_{1/2})^1$, 46.366% $(1p_{3/2})^5$ $(1p_{1/2})^0$, and 2.520% $(1p_{3/2})^1$ $(1p_{1/2})^4$, as shown in Fig. (1). The calculated elastic transverse form factors for the ground state of ^{9}Be nucleus (using b_{rms} = 1.6178 fm) with *p*-shell model space (MS) are displayed in Fig. (2) with M1 and M3 transitions. The E2 form factor was negligibly small. The calculated transverse form factors (solid curve) were compared with the data reported by Glickman et al. [17], Lapikas et al. [22] and Rand et al. [23]. While the separate contributions are displayed for M1(dashed curve) and M3 (dashed-dot curve) parts. It is evident that the M3 contribution dominated along the range of momentum transfer ($0.5 < q < 3.0$) fm^{-1}, while at low q-value (q~1.0 fm^{-1}) the M1 contribution (first maximum) was the most significant, with diffraction minimum located at q~1.3 fm^{-1}, which is a reasonable compared with the experimental region (at q~1.1 fm^{-1}).

The experimental data cannot be reproduced with free g-factor and was underestimated along all region of momentum transfer. The effect of the center of mass correction slightly reduced these discrepancies especially at high q-value, as shown in Fig. (3) (green curve). The value of magnetic dipole-moment for this transition is μ = -1.266 n.m. with g(free), which is higher than the measured value of $\mu_{exp.}$ = -1.1778(9) n.m. [24]. Inclusion of the core polarization effects through the effective g-factors for proton and neutron with the values of $g_l^p = 0.9, g_l^n = 0.0, g_s^p = 5.5857, g_s^n = -3.4436$ changed the value of magnetic moment to μ = -1.178 n.m. and gave the best agreement with the measured value. This result is very close to that of Tomaselli et al. [25], their calculated value was μ = -1.18 n.m. using the microscopic dynamic-correlation model (DCM), which is different from that of Cravo [26] by a factor of 2. This comparison is listed in Table (I). The contributions of higher 2*p*-shell configuration (with δ = γ = -0. 95) together with $g_{eff.}$ can very well reproduce the data at low region of q as shown in Fig. (4) (red curve). The calculated transverse form factors described extremely well the general behavior of the experimental points over whole regions of momentum transfer, as shown in Fig. (5). The same behavior was given by Cravo [26], but their results were lower than the data. The reason of the discrepancy at high q-region is that in high q-region, the large momentum virtual photon may excite more degrees of freedom such as, Δ- isobar, and even quark structure of hadrons, and more than one particle may share the momentum transfer carried by the virtual photon.

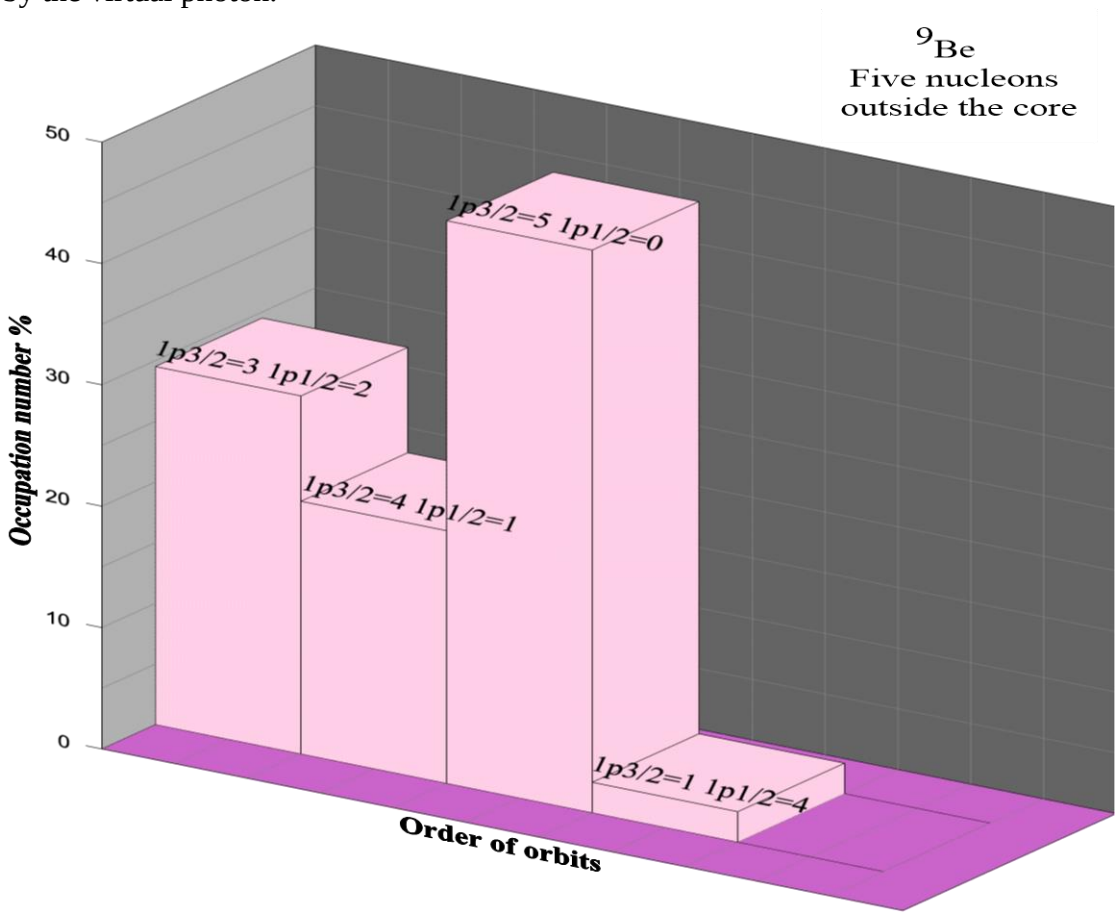

Figure 1- The percentage of the occupation numbers for the ground states of $1p_{3/2}$, $1p_{1/2}$ orbits outside the ^{4}He core of considered ^{9}Be nucleus.

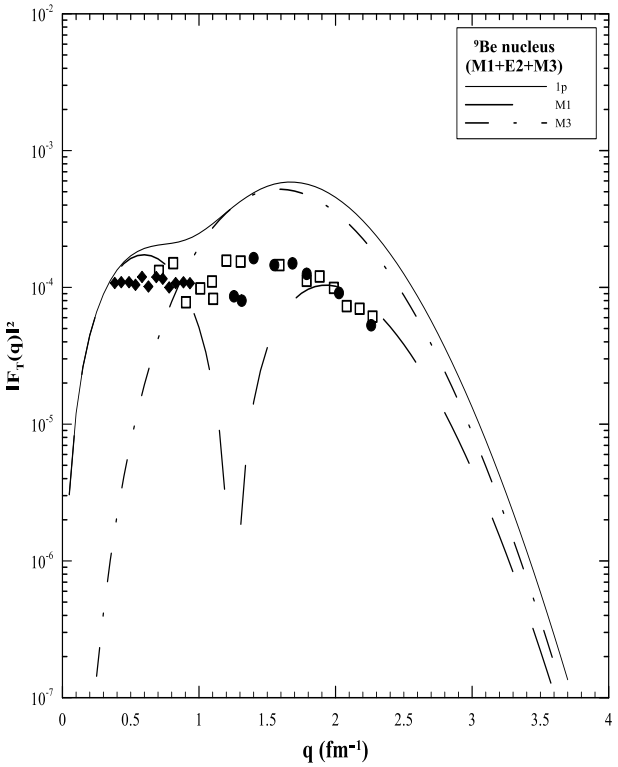

Figure 2-The transverse form factors of ^{9}Be ground state calculated in *p*-model space. The individual multipole contribution of M1 and M3 are shown. The data are taken from Ref. [17] (circles), Ref. [22] (diamond) and Ref. [23] (square).

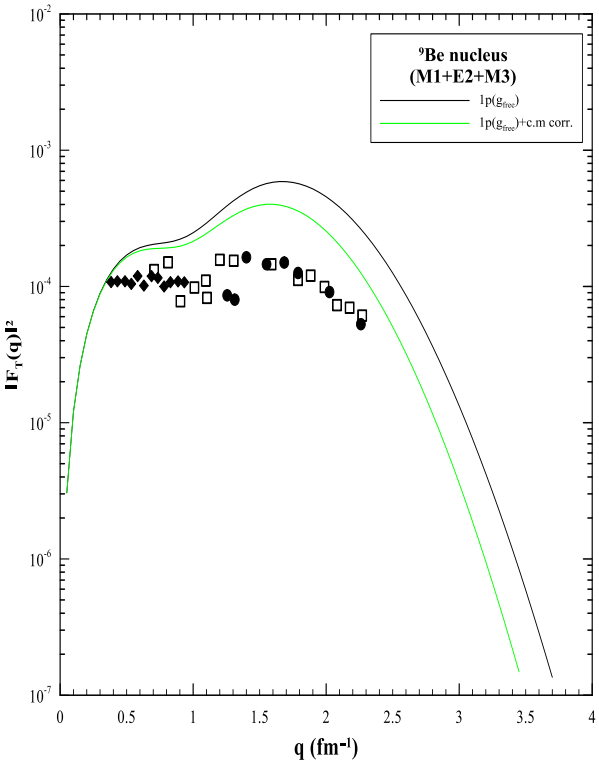

Figure 3-Comparison between the total form factors of ^{9}Be nucleus with $g_{(free)}$ (black curve), and with $g_{(free)}$+c.m. corr. (green curve). The data are the same as in Fig. (3.1).

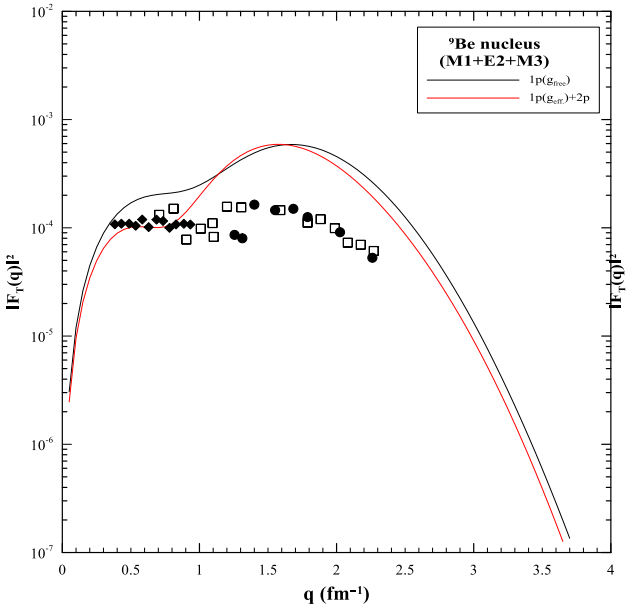

Figure 4-Comparison between the total form factors of ^{9}Be nucleus with $g_{(free)}$ (black curve), and with $g_{(eff.)}$ +2p (red curve). The data are the same as in Fig. (1).

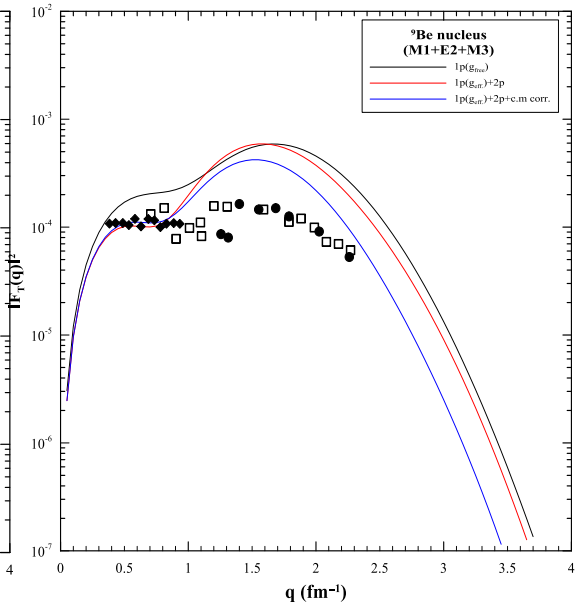

Figure 5- Comparison between the total form factors of ^{9}Be nucleus with $g_{(free)}$ (black curve), with $g_{(eff.)}$ +2p (red curve) and with $g_{(eff.)}$ +2p+c.m. corr. (blue curve). The data are the same as in Fig. (1).

3.2 ^{7}Be nucleus ($J^{\pi}T = 3/2^{-}1/2$, $\tau_{1/2} = 53.3$ d)

The ground state of ^{7}Be exotic nucleus can be regarded as a core of ^{4}He with three nucleons distributed over $1p_{3/2}$ and $1p_{1/2}$ orbits. The $(1s)^4$ inert core, $(1p)^3$ configurations for the ground state of ^{7}Be were used with C-K interaction [12]. This results in a clear configuration mixture with, 21.671% $(1p_{3/2})^2$ $(1p_{1/2})^1$, 52.739% $(1p_{3/2})^3$ $(1p_{1/2})^0$, and 25.589% $(1p_{3/2})^1$ $(1p_{1/2})^2$, as shown in Fig. (6). The single particle wave functions of HO potential, with size parameter b = 1.5767 fm were used. The elastic transverse form factors for 1*p*-shell model space of ^{7}Be nucleus had a good behavior compared with that of a stable ^{9}Be nucleus, as depicted in Fig. (7) (solid curve). The individual components M1 (dashed curve) and M3 (dashed-dot curve) were indicated. The E2 form factor was negligibly small. The M3 contribution dominated around q~1.7 fm^{-1} region, while the first maximum of M1 contribution had almost the same location of the diffraction minimum as that of the ^{9}Be nucleus (at q~1.3 fm^{-1}). The contribution of the center of mass correction reduced the transverse form factors at high range of momentum transfers to be closer to the data, as shown in Fig. (8) (green curve). The value of magnetic dipole moment with free g-factor was μ = -1.287 n.m., which is less than the measured value of $\mu_{exp.}$ = -1.398(15) n.m. [24]. The role of effective g-factors with $g_l^p = 0.81$, $g_l^n = 0.0$, $g_s^p = 5.5857$, $g_s^n = -3.8263$, was restricted to reproduce very well the measured value of magnetic moment of μ = -1.399 n.m. This value is less than that reported by Marcucci et al. [5], as shown in Table (I). The inclusion of higher 2*p*-shell mixture (with $\delta = \gamma = 0.998$) with effective g-factors had minor effect on the form factors along all range of q, as shown in Fig. (9) (red curve). The blue curve in Fig. (10) represents the calculations including the contributions of the center of mass correction with 2*p*-shell and effective g-factors. The calculated transverse form factors for both ^{7}Be and ^{9}Be were quite similar.

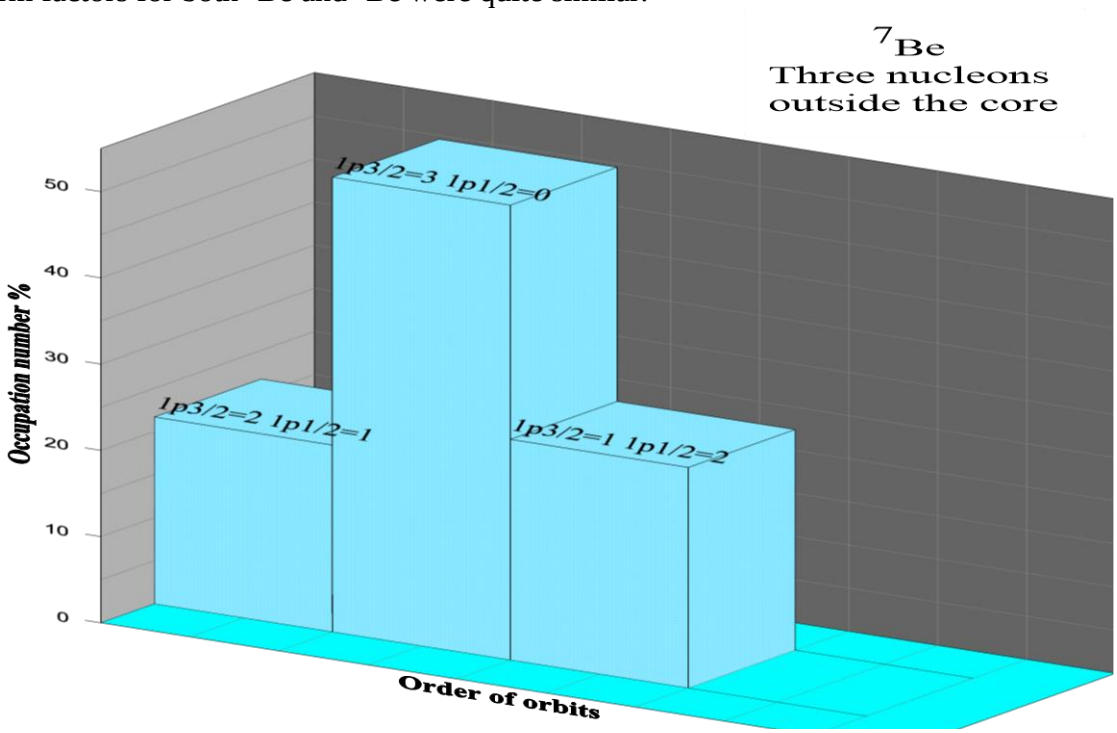

Figure 6- The percentage of the occupation numbers for the ground states of $1p_{3/2}$, $1p_{1/2}$ orbits outside the ^{4}He core of considered ^{7}Be nucleus.

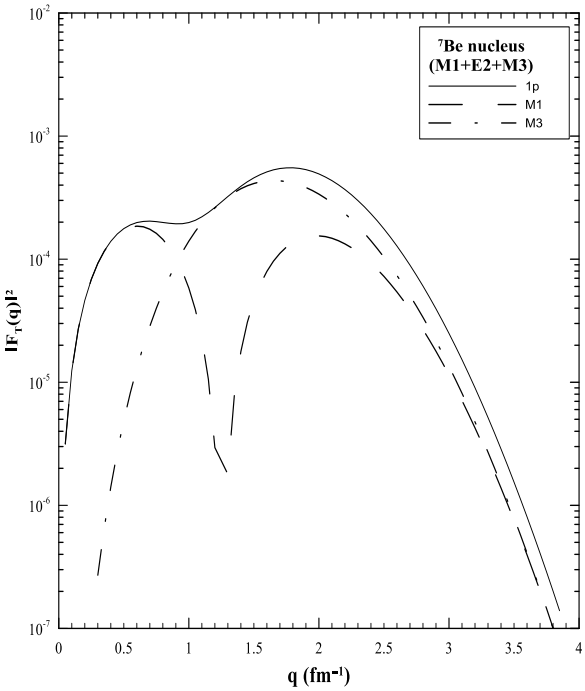

Figure7-The transverse form factors for ^{7}Be ground state calculated in *p*-model space. The individual multipole contribution of M1 and M3 are shown.

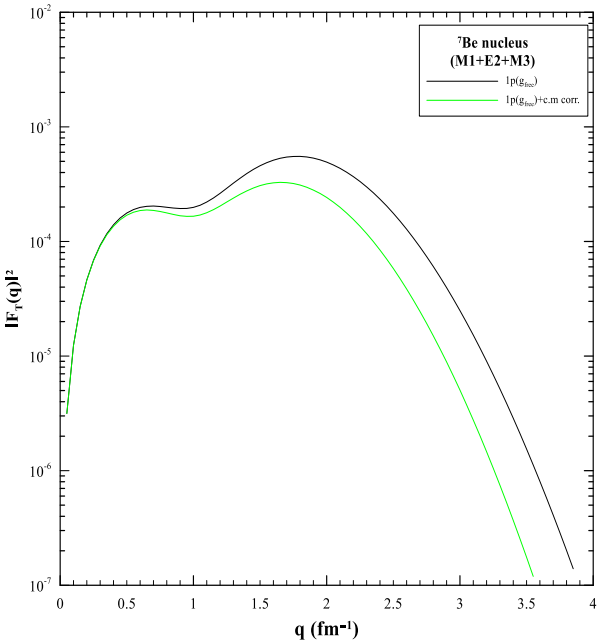

Figure 8-Comparison between the total form factors of ^{7}Be nucleus with $g_{(free)}$ (black curve), and with $g_{(free)}$+c.m. corr. (green curve).

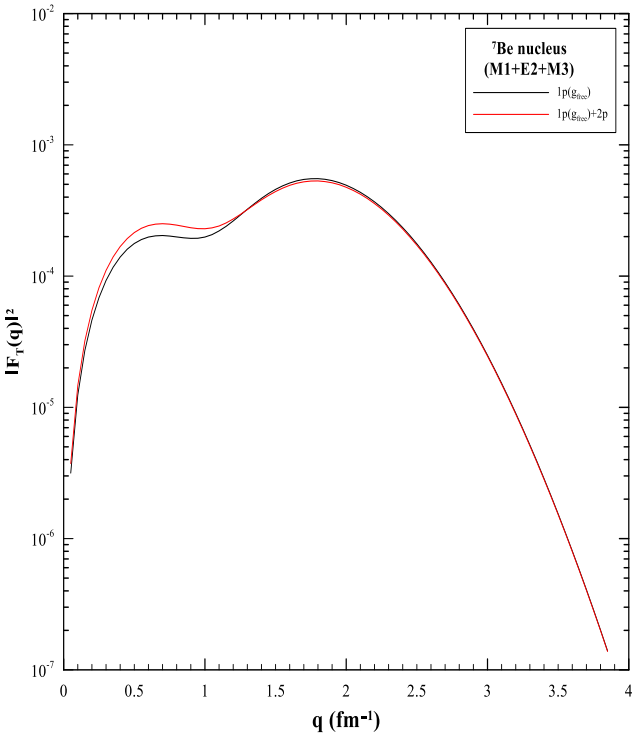

Figure 9- Comparison between the total form factors of ^{7}Be nucleus with $g_{(free)}$ (black curve), and with $g_{(eff.)}$ +2p (red curve).

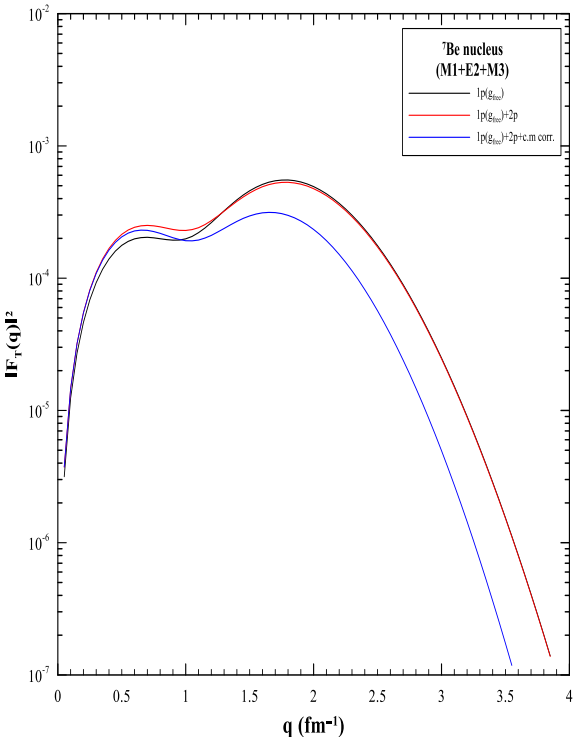

Figure 10- The total form factors of the ^{7}Be nucleus, with $g_{(free)}$ (black curve) are compared with $g_{(eff.)}$ +2p (red curve) and with $g_{(eff.)}$ + 2p+c.m. corr. (blue curve).

3.3 ^{11}Be nucleus ($J^{\pi}T = 3/2^{-}3/2$, $\tau_{1/2}$=13.8 s)

The ground state of exotic ^{11}Be nucleus (neutron rich) is specified by $J^{\pi}T = 3/2^{-}$ 3/2, with a half-life time of $\tau_{½}$ = 13.8 s, so the experimental information on this state is very scarce. The ground state of ^{11}Be has the configurations of $(1s)^4$ inert core, $(1p)^7$ with C-K interaction [12]. A clear configuration mixture in this state appeared with, 41.698% $(1p_{3/2})^5$ $(1p_{1/2})^2$, 01.531% $(1p_{3/2})^4$ $(1p_{1/2})^3$, 51.948% $(1p_{3/2})^6$ $(1p_{1/2})^1$, and 04.824% $(1p_{3/2})^3$ $(1p_{1/2})^4$, as shown in Fig. (11). The calculated transverse form factors for *p*-shell model space with C-K interaction are shown in Fig. (12) (solid curve). The individual components M1 (dashed curve) and M3 (dashed-dot curve) are indicated. It is worth noting that the E2 form factor was negligibly small. The M3 component dominated around q~1.5 fm^{-1} region, while the M1 component was slightly shifted backward with the location of the diffraction maximum around q~0.9 fm^{-1}. The single particle wave functions of HO potential were used with size parameter b = 1.6534 fm. The inclusion of center of mass correction made reduction in the magnetic form factors at high q-value, as shown in Fig. (13) (green curve). The admixture of higher 2*p*-shell contributions with core polarization effects gave some enhancement in the height of the form factors at low q-region, this was indicated in Fig. (14) (red curve). In general, the results were modified when the center of mass correction was included, as shown in Fig. (15) (blue curve).

The value of magnetic dipole moment for g-free was μ = -0.972 n.m., which was less than the measured value of $\mu_{exp.}$ = -1.6814(13) n.m. [24]. Inclusion of $g_{\text{-eff.}}$ for proton and neutron with the values of $g_l^p = 1.649$, $g_l^n = 0.64$, $g_s^p = 9.1605$, $g_s^n = -6.2751$, modified the value of magnetic moment to μ = -1.683 n.m. This result has a very good agreement with the measured value.

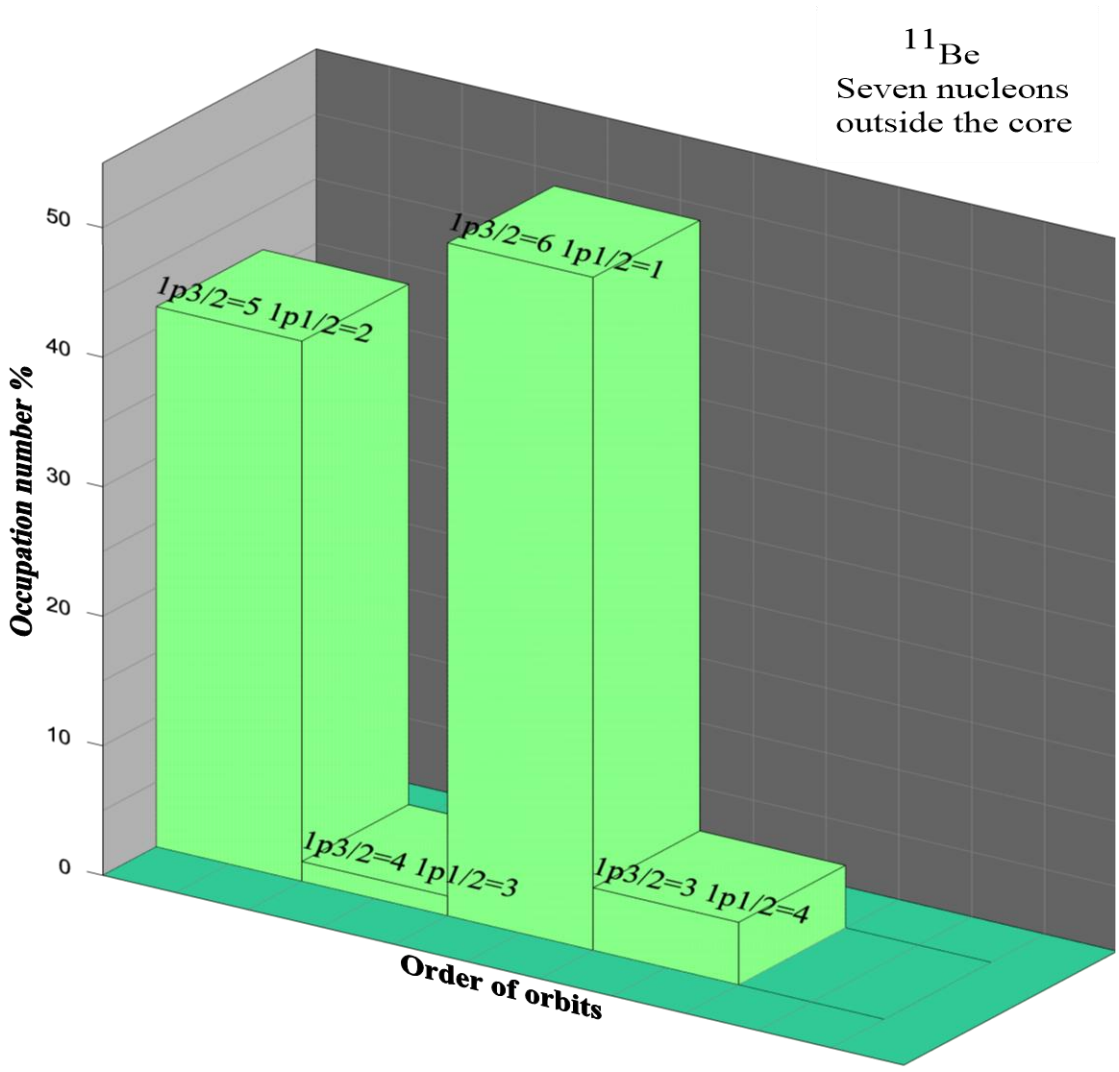

Figure 11-The percentage of the occupation numbers for the ground states of $1p_{3/2}$, $1p_{1/2}$ orbits outside the ^{4}He core of considered ^{11}Be nucleus.

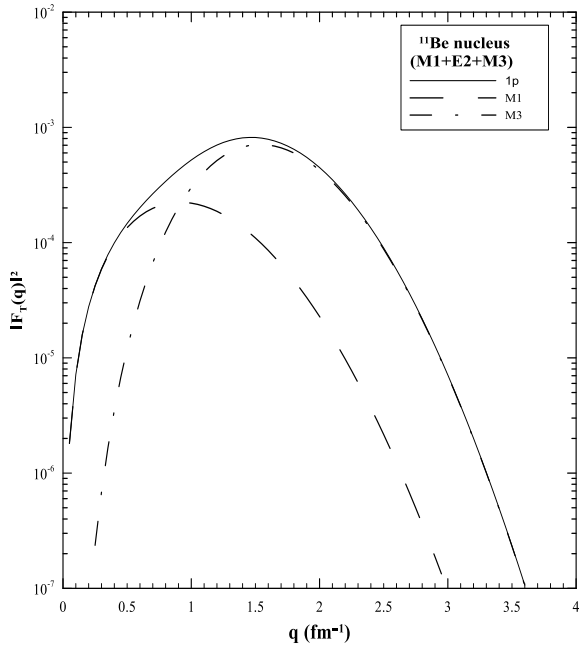

Figure 12-The transverse form factors for ^{11}Be ground state calculated in *p*-model space. The individual multipole contribution of M1 and M3 are shown.

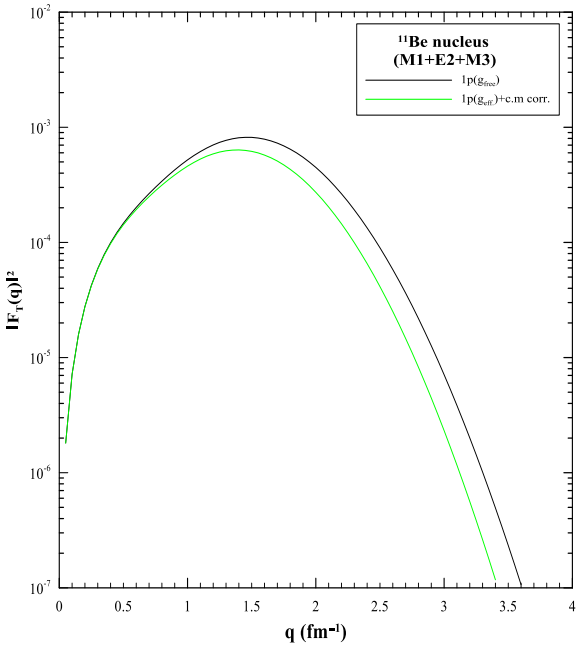

Figure 13-Comparison between the total form factors of ^{11}Be nucleus with $g_{(free)}$ (black curve), and with $g_{(free.)}$ +c.m. corr. (green curve).

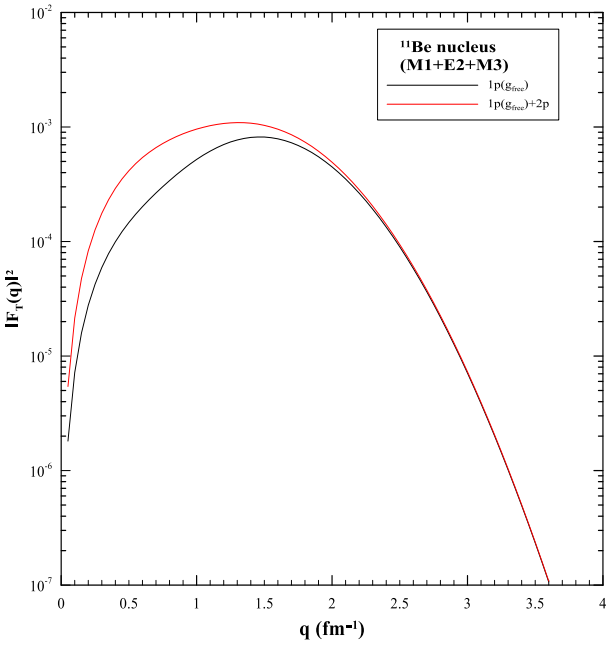

Figure 14-The total form factors of ^{11}Be nucleus with $g_{(free)}$ (black curve) are compared with $g_{(eff.)}$ +2p (red curve).

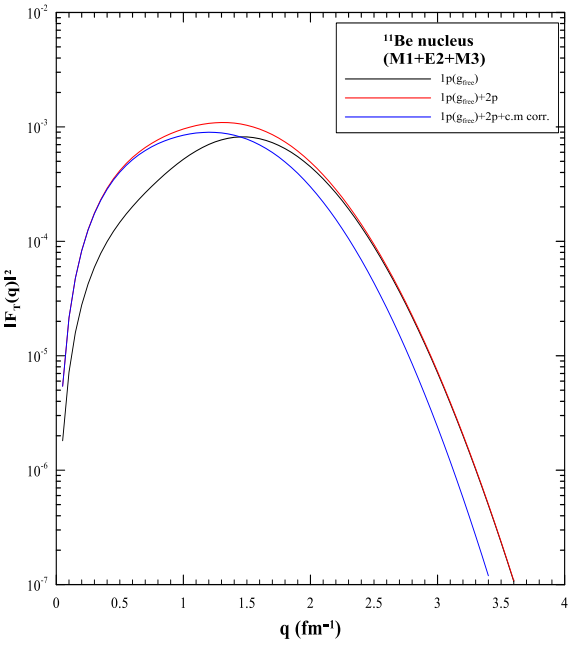

Figure15-Comparison between the total form factors of ^{11}Be nucleus with $g_{(free)}$ (black curve), with $g_{(eff.)}$ +2p (red curve) and with $g_{(eff.)}$ +2p+c.m. corr.

The comparison of the calculated total transverse form factors of ^{7}Be (red curve), ^{9}Be (black curve) and ^{11}Be (blue curve) as well as with the experimental data of stable nucleus ^{9}Be [17,22,23] are shown in Fig. (16). The transverse form factors of ^{7,9}Be nuclei were quite similar to each other and different from that of ^{11}Be. They had the same behavior with well description of the experimental data especially at low q-region ($q \leq 1.5$ fm^{-1}), and still slightly overestimated the data at high q-value. The closer form factors (in shape) of ^{7,9}Be nuclei in all q-regions mean that the tail part of the wave functions of the last neutron in ^{7,9}Be nuclei are close to each other when the last neutron occupies the same orbital (here $P_{3/2}$ orbit). This can be deduced from the comparison between the shapes of both form factors with experimental data.

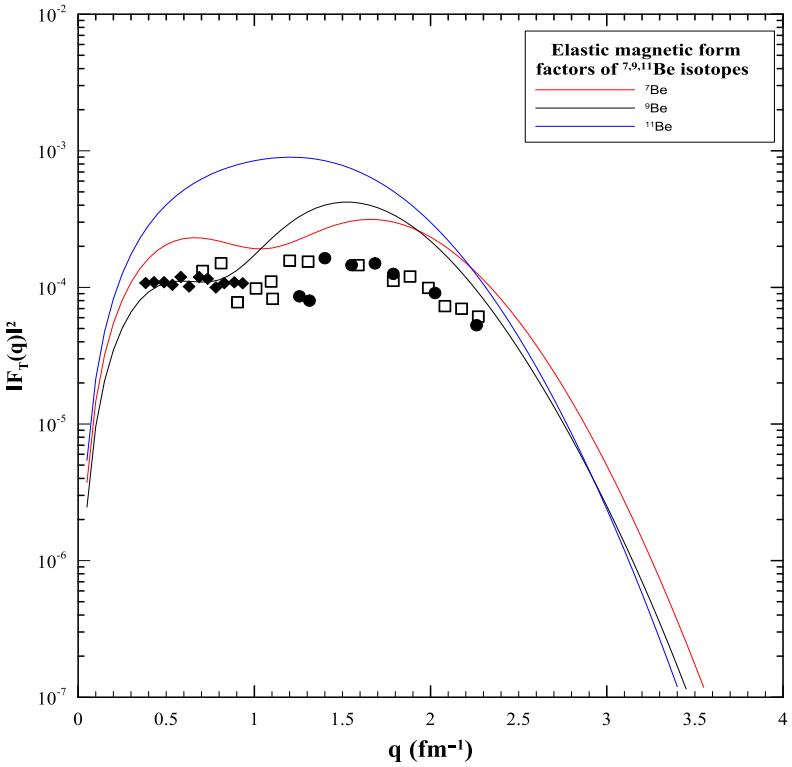

Figure 16- Comparison between the total elastic magnetic form factors of ^{7,9,11}Be isotopes using the $g_{eff.}$ +2p+c.m. corr. with experimental data of ^{9}Be nucleus taken from Glickman et al. [17] (circles), Lapikas et al. [22] (diamond) and Rand et al. [23] (square).

Table 1- The calculated magnetic dipole moments (μ) of ^{7,9,11}Be isotopes are compared with experimental data of Ref. [24] and with other results.

Nucleus	$J^{\pi}T$	***g*(free)**	***g*(eff.)**	$\mu_{exp.}$ **(*n m*)**	***Other results***
^{7}Be	$3/2^{-}$ 1/2	-1.287	-1.399[(a)]	-1.398(15)	-1.493(15)[5]
^{9}Be	$3/2^{-}$ 1/2	-1.266	-1.178[(b)]	-1.1778(9)	-1.18[25] -1.151[26]
^{11}Be	$3/2^{-}$ 3/2	-0.972	-1.683[(c)]	-1.6814(13)	-1.705[27]

(a) $g_l^p = 0.81.\ g_l^n = 0.0.\ g_s^p = 5.5857.\ g_s^n = -3.8263$

(b) $g_l^p = 0.9.\ g_l^n = 0.0.\ g_s^p = 5.5857.\ g_s^n = -3.4436$

(c) $g_l^p = 1.64.\ g_l^n = 0.64.\ g_s^p = 9.1605.\ g_s^n = -6.2751$

4. Conclusions

The main conclusions for the current work can be drawn in the following:

1. Effective g-factors have minor effect on the form factors along all range of q, and a major effect on the magnitude of magnetic dipole moments.
2. The only distinction is due to the difference in the center of mass correction between the transverse form factors of the stable nucleus and that of the unstable nucleus.
3. For ^{7,9}Be nuclei, the form factors are quite similar to each other and different from that of ^{11}Be.
4. The present results of ^{7,9}Be nuclei are successful in describing the low q-region behavior, and still overestimated at high q-data.
5. At high q-region, the large momentum virtual photon may excite more degrees of freedom such as, even quark structure of hadrons, Δ- isobar, and more than one particle may share the momentum transfer carried by the virtual photon. This reason is sufficient to create the discrepancy at high q-region.
6. Analysis calculations of ^{7,9,11}Be isotopes with the present occupation numbers, show a strong contribution of $1p_{3/2}$ orbit and a clear exotic behavior for the valence nucleons of ^{11}Be.

5. References

[1] J. D. Walecka, "Overview of the CEBAF Scientific program", *A.I.P. Con. Proc*., vol. 269, no. 87, 1992, eds. F. Gross and R. Holt, A.I.P., New York, 97 (1993).

[2] I. Tanihata et al., *Phys. Rev. Lett*., vol. 55, no. 2676, 1985.

[3] K. Hagino, I. Tanihata, and H. Sagawa, in "*100 Years of Subatomic Physics*", *edited by E. M. Henley and S. D. Ellis*, (*World Scientific, Singapore*), pp. 231-272, (2013).

[4] R. Palit, P. Adrich, T. Aumann, K. Boretzky, B. V. Carlson, D. Cortina, U. Datta Pramanik, Th. W. Elze, H. Emling, H. Geissel, M. Hellstro, K. L. Jones, J. V. Kratz, R. Kulessa, Y. Leifels, A. Leistenschneider, G. Münzenberg, C. Nociforo, P. Reiter, H. Simon, K. Sümmerer and W. Walus (LAND/FRS Collaboration), *Phys. Rev. C*, vol. 68, pp. 034318, 2003.

[5] L. E. Marcucci, Muslema Pervin, Steven C. Pieper, R. Schiavilla and R. B. Wiringa, *Phys. Rev. C*, vol. 78, no. 6, pp. 065501, 2008.

[6] T. Dong and Z. Ren, *Chin. Phys. Lett*., vol. 25, no. 3, pp. 884, 2008.

[7] H. W. Hammer and D. R. Phillips, *Nucl. Phys. A*, vol. 847, pp. 1-23, 2010.

[8] J. C. Zamora, V. Guimarães, A. barioni, A. Lépine-Szily, R. Lichtenthäler, P. N. de Fria, D. R. Mendes Jr., L. R. Gasques, J. M. B. Shorto, V. Scarduelli, K. C. C. Pires, V. Morcelle, E. Leistenschneider, R. P. Condori, V. A. Zagatto, M. C. Moraisand E. Crema, *Phys. Rev. C*, vol. 84, pp. 034611, 2011.

[9] H. T. Fortune, *Eur. Phys. J. A*, vol. 54, no. 51, 2018.

[10] P. Sarriguren, D. Merino, O. Moreno, E. Moya de Guerra, D. N. Kadrev. A. N. Antonov and M. K. Gaidrov, *Phys. Rev. C*, vol. 99, pp. 034325, 2019.

[11] P. Sarriguren, O. Moreno, E. Moya de Guerra, D. N. Kadrev. A. N. Antonov and M. K. Gaidrov, *J. of Physics: Conference Series*, vol. 1555, 2020, 012001.

[12] S. Cohen and D. Kurath, *Nucl. Phys*., vol. 73, no. 1, 1965.

[13] Bogdan Mihaila and Jochen H. Heisenberg, *Phys. Rev. C* , vol. 60, pp. 054303, 1999, *Phys. Rev. C*, vol. 61, pp. 054309, 2000, and *Phys. Rev. Lett*., vol. 84, no.1403, 2000.

[14] T. W. Donnelly and I. Sick, *Rev. Mod. Phys*., vol. 56, no. 461, 1984.

[15] P. J. Brussaard and P. W. M. Glademans, "*Shell-Model Application in Nuclear Spectroscopy*", *North-Holland Publishing Company, Amsterdam*, 1977.

[16] B. A. Brown, A. Etchgoyen, N. S. Godwin, W. D. M. Rae, W. A. Richter, W. E. Ormand, E. K. Warburton, J. S. Winfield, L. Zhao and C. H. Zimmerman, MSU-NSCL report number 1289, 2005.

[17] J. P. Glickman, W. Bertozzi, T. N. Buti, S. Dixit, F. W. Hersman, C. E. Hyde-Wright, M. V. Hynes, R. W. Lourie, B. E. Norum, J. J. Kelly, B. L. Berman, and D. J. Millener, *Phys. Rev. C*, vol. 43, no. 1740, 1991.

[18] L. J. Tassie and F. C. Barker, *Phys. Rev*. vol. 111, no. 940, 1958.

[19] A. A. Abdullah, R. A. Radhi and Z. A. Dakhil, *Indian J. Phys. 75A*, vol. 579, 2001.

[20] I. S. Towner, *Oxford Studies in Nuclear Physics, Clarendon press, Oxford*, 1971.

[21] B. A. Brown, R. A Radhi and B. H. Wildenthal, *Phys. Rep*. vol. 101, no. 313, 1983.

[22] L. Lapikas, G. Box and H. deVries, *Nucl. Phys. A* , vol. 253, no. 324, 1975.

[23] R. E. Rand, R. Frosch and M. R. Yearian, *Phys. Rev*. vol. 144, no. 3, 859, 1966.

[24] N. J. Stone, "Table of nuclear magnetic dipole and electric quadrupole moments", *International Data Committee, International Atomic Energy Agency* (IAEA), INDC (NDS), 0658, 2014.

[25] M. Tomaselli, L. C. Liu, S. Fritzsche, T. Kuhl and D. Ursescu, *Nucl. Phys. A* , vol. 738, no. 216, 2004.

[26] E. Cravo, *Phys. Rev. C* , vol. 54, no. 2, pp. 523, 1996.

[27] Toshio Suzuki, Rintaro Fujimoto, Takaharu Otsuka, *Phys. Rev. C*, vol. 67, *pp.*044302, 2003.